Free convection of nanoliquids in an enclosure with sinusoidal heating

S. Sivasankaran[1,*] T. Aasaithambi[2], M. Bhuvaneswari[1], S. Rajan[3]
[1]Department of Mathematics, King Abdulaziz University, Jeddah, Saudi Arabia
[2]Department of Mathematics, Sri Shanmugha College of Engineering and Technology, Pullipalayam, Sankari, Tamilnadu, India
[3]Department of Mathematics, Erode Arts and Science College, Erode, Tamilnadu, India
[*]Corresponding author email: sd.siva@yahoo.com; sdsiva@gmail.com.

Abstract. The goal of the current numerical research is to explore the convection of different nanoliquids in a square cavity. The temperature at left wall varies sinusoidally whereas the temperature at right wall is kept as constant. The horizontal walls are taken as adiabatic. The finite volume method is utilized to discretize the governing equations and the solutions are found iteratively for diverse combinations of relevant parameters involved in the study. It is established that the energy transfer enhances with raising the nanoliquid volume fraction. The growth in the averaged energy transport strongly depends on the nanoparticle chosen.

1. Introduction

Convective cooling augmentation method has been a key problem in many industrial and technological applications because of thermal controlling of devices. In recent years, nanoliquids are considered in heat transfer research to analyze the number of factors in different ways. Ho *et al*. [1] numerically examined the properties of nanoliquids on convection in the enclosure. Sivasankaran et al. [2] numerically examined the free convection of nanoliquids in an enclosed space with linearly heated wall. Ho et al. [3] experimentally investigated the free convection of nanoliquid in a vertical enclosure. The thermophoresis, sedimentation, and Brownian motion effects on Rayleigh–Bénard free convection of nanoliquids in an enclosed space were examined by Ho et al. [4].

The maximum number of the reports on convection of nanoliquids in cavities have been considered either isoflux and/or isothermal thermal conditions in boundaries. But, these temperature conditions at boundary are not appropriate in numerous applications. Therefore, we want the awareness of the outcome of non-isothermal wall temperature to analyze several applications. The non-uniform heating effect on both walls in a cavity was examined by Sivasankaran et al. [5]. The MHD convection in cavities with non-uniform boundary heating was examined by several authors [6-7]. Convection in a porous enclosed space with sinusoidal boundary heating on side walls was reported in Ref. [8-9]. The aspect ratio and inclination effects on free convection with sinusoidal surface condition was explored by Cheong et al. [10]. Sivasankaran and Pan [11] numerically examined the free convection of nanoliquids with sinusoidal heating walls. The non-uniform temperature on sidewall(s) in a cavity under different situations is examined by several authors in different studies [12-16].

No work has been executed on convection flow of nanoliquids for non-uniform boundary conditions with different nanoliquids. Hence, the present report aims to explore the effects of free convection characteristics with sinusoidally varying wall temperature utilizing different nanoliquids.

2. Mathematical Modelling

A two-dimensional enclosed space of height L filled with water-based nanoliquids containing various nano-particles (Al_2O_3, Cu, Ag and TiO_2) is taken for examination as displayed in the Figure 1. The vertical left wall is sinusoidally heated and the vertical right wall is cooled at a uniform temperature. The bottom & top boundaries are adiabatic. The nanoliquid is a liquid-solid blend with uniform shape, size, and volume fraction of nano-particles distributed within base liquid water. The flow is presumed to be incompressible and laminar. It is presumed that both water and nano-particles are in thermally equilibrium. The buoyancy term based on Boussinesq approximation is added and other thermo-physical properties are expected to be constant. It is presumed that no chemical reaction between the nanoparticles and water. The mathematical model for the above said geometrical and physical conditions can be written as follows.

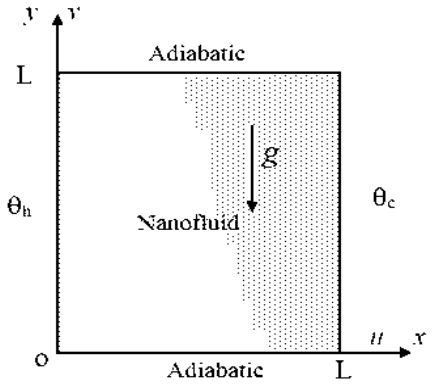

Fig. 1. Physical configuration

$$u_x + v_y = 0 \tag{1}$$

$$u_t + uu_x + vu_x = -(1/\rho_{nf})p_x + (\mu_{nf}/\rho_{nf})[\nabla^2 u] \tag{2}$$

$$v_t + uv_x + vv_x = -(1/\rho_{nf})p_y + (\mu_{nf}/\rho_{nf})[\nabla^2 v] + (g(\rho\beta)_{nf}/\rho_{nf})(\theta - \theta_c) \tag{3}$$

$$\theta_t + u\theta_x + v\theta_y = \alpha_{nf}[\nabla^2 \theta] \tag{4}$$

The no-slip velocity conditions are taken on all walls. The temperature on left and right walls are taken as θ = sin(y/L) and $\theta = 0$. The thermo-physical properties of the nanoliquid calculated using several formulae are as follows.

$$\rho_{nf} = \phi\rho_p + (1-\phi)\rho_f$$

$$(\rho\beta)_{nf} = \phi(\rho\beta)_p + (1-\phi)(\rho\beta)_f$$

$$(\rho c_p)_{nf} = \phi(\rho c_p)_p + (1-\phi)(\rho c_p)_f$$

$$k_{nf} = k_f\left[\frac{2\phi(k^*_{pf}-1) + k^*_{pf} + 2}{k^*_{pf} - \phi(k^*_{pf}-1) + 2}\right] \quad \text{with} \quad k^*_{pf} = k_p/k_f$$

$$\mu_{nf} = \mu_f(1-\phi)^{-2.5}$$

The properties of the water and various nano-particles are found in (Ho et al., 2008). The dimensionless variables are derived as follows.

$$(U,V) = (u,v)L/\alpha_{nf},\ (X,Y) = (x,y)/L,\ T = \frac{\theta - \theta_c}{(\theta_h - \theta_c)},\ F_0 = \frac{t\alpha_{nf}}{L^2},\ \text{and}\ P = \frac{pL^2}{\rho_{nf}\alpha_{nf}^2}.$$

Using this non-dimensional variables, the equations are non-dimensionalized and they are given as follows:

$$\frac{\partial U}{\partial X} + \frac{\partial V}{\partial Y} = 0 \tag{5}$$

$$\frac{\partial U}{\partial F_O} + U\frac{\partial U}{\partial X} + V\frac{\partial U}{\partial Y} = -\frac{\partial P}{\partial X} + \Pr_f\left(\frac{C^*_{p,nf}\mu^*_{nf}}{k^*_{nf}}\right)\left[\frac{\partial^2 U}{\partial X^2} + \frac{\partial^2 U}{\partial Y^2}\right] \tag{6}$$

$$\frac{\partial V}{\partial F_O} + U\frac{\partial V}{\partial X} + V\frac{\partial V}{\partial Y} = -\frac{\partial P}{\partial Y} + \Pr_f\left(\frac{C^*_{p,nf}\mu^*_{nf}}{k^*_{nf}}\right)\left[\frac{\partial^2 V}{\partial X^2} + \frac{\partial^2 V}{\partial Y^2}\right] + Ra_f\,\Pr_f\,\beta^*_{nf}\left(\frac{\rho^*_{nf}C^*_{p,nf}}{k^*_{nf}}\right)^2 T \tag{7}$$

$$\frac{\partial T}{\partial F_O}+U\frac{\partial T}{\partial X}+V\frac{\partial T}{\partial Y}=\left[\frac{\partial}{\partial X}\left(k_{nf}^{*}\frac{\partial T}{\partial X}\right)+\frac{\partial}{\partial Y}\left(k_{nf}^{*}\frac{\partial T}{\partial Y}\right)\right] \tag{8}$$

The surface conditions in the non-dimensional form are as follows. No slip condition for velocity on side walls. The left and right walls temperature are taken as T = sin(Y) and T=0.

The physical properties ratios appear in equations (2-4) are as follows. $k_{nf}^{*}=k_{nf}/k_f$, $\mu_{nf}^{*}=\mu_{nf}/\mu_f$, $Cp_{nf}^{*}=Cp_{nf}/Cp_f$, $\rho_{nf}^{*}=\rho_{nf}/\rho_f$, and $\beta_{nf}^{*}=\beta_{nf}/\beta_f$, where the subscripts *nf* and *f* denote the nanoliquid and water. The non-dimensional numbers performed in the above equations are, $Ra_f=\frac{g\beta_f(\theta_h-\theta_c)L^3}{\nu_f\alpha_f}$, Rayleigh number, and $\mathrm{Pr}_f=\frac{\nu_f}{\alpha_f}$, Prandtl number (Pr=6.7). The stream function is defined by $U=\frac{\partial\Psi}{\partial Y}$ and $V=-\frac{\partial\Psi}{\partial X}$.

The energy transfer rate at the heated surface is obtained by the Nusselt number, which is estimated as $Nu_h=\frac{h_nL}{k_f}=-k_{nf}^{*}\left.\frac{\partial T}{\partial Y}\right|_{X=0}$. The averaged Nusselt number along the heated surface is acquired as $\overline{Nu}=\int_0^1 Nu_h dY$. Moreover, it is also significant to enumerate the energy transport efficacy of using the nanoliquid to that of the water. The averaged energy transfer coefficient ratio of nanoliquid to that of the water, ε_h, is computed as $\varepsilon_h=\overline{h_n}/\overline{h_f}$. The solution of the dimensionless governing systems are done by finite volume method. The detailed solution methodology is found in Ref. Sivasankaran et al. (2010).

3. Results and Discussion

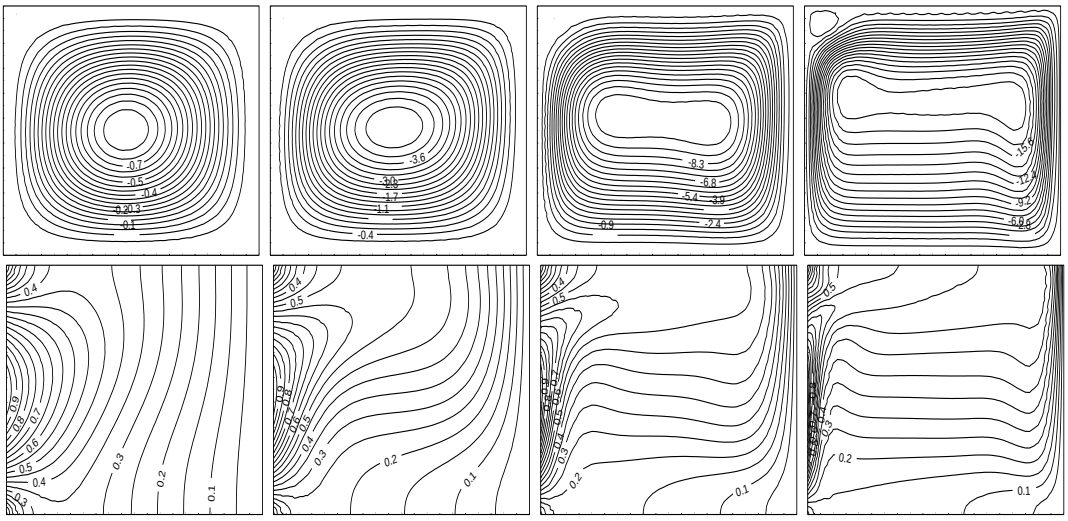

(a) *Ra*=10^3 (b) Ra=10^4 (c) Ra=10^5 (d) Ra=10^6

Fig. 2. Streamlines (up) and isotherms (down) of Al_2O_3-nanofluid with ϕ=4% for various Ra.

The calculations are done for the Rayleigh numbers from 10^3 to 10^6, and the volume fraction ϕ of nano-particles from 0% to 4%. Figure 2 displays liquid stream and temperature characteristics of Al_2O_3-nanofluid for different Rayleigh numbers. The stream pattern is involves a cell occupying the complete enclosure. The core area of the cell is at central part of the cavity for the weak buoyancy force ($Ra=10^3$). The isotherms are spread equally inside the cavity. Here energy transport is by means of conduction dominated mode. When increasing Ra, the core area of the cell elongated horizontally ($Ra\geq10^5$). The minor cell exists in the high values of Rayleigh number at the left-top corner due to non-uniform heating. The isotherms illustrate the vertical stratification of temperature in the cavity. The isotherms are crowded beside the thermal walls and forming the thermal boundary layers. It clearly indicates that convection mode of heat transfer is dominated here.

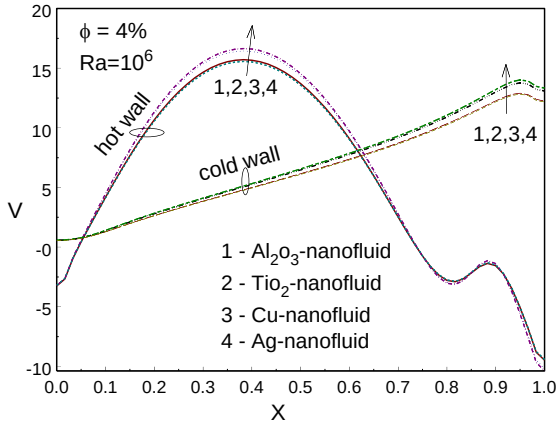

Fig. 3. Local Nusselt number for various nanofluids with $Ra=10^6$ and ϕ=4%.

The effect of local energy transfer rate among the different nanofluid is displayed in Figure 3. It is witnessed that the higher energy transfer is gained when using Ag-nanoliquid. A further inspection of the profiles exposes that the highest value of local energy transfer rate is achieved at Y=0.35 for $Ra=10^6$, that is ¼ from the bottom of the warmer wall. It is witnessed that the highest local energy transport rate is achieved at the middle part of left wall for sinusoidally varying wall temperature and at the top of the wall for isothermal surface temperature. The wavy shape of local Nusselt number profile indicates the direct effect of non-uniform heating of sidewall on energy transfer.

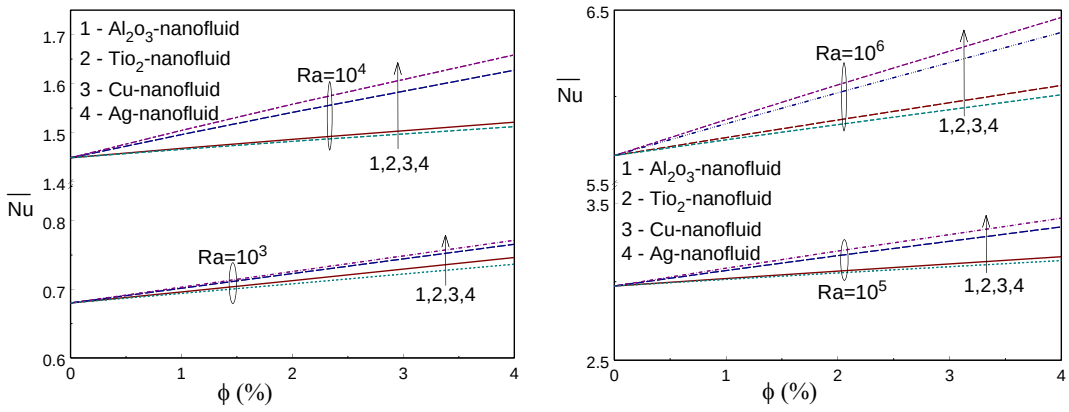

Fig. 4. Averaged Nusselt number for various volume fractions and nanofluids.

Figure 4 provides the effect of total energy transport rate through the enclosure among the various nanoliquids. The favorable effects of the nano-particle fraction on the averaged Nusselt number trend can be perceived clearly with raising the particle fraction. Averaged Nusselt number enhances on raising the values of Ra. It is established that the maximum energy transfer rate is witnessed for using Ag-nanoparticle comparing among other nanoparticles, like Cu, Al_2O_3 and TiO_2. When raising the nanoliquid volume fraction, the variation in the energy transport rate amongst the various nanoliquids is increased. The change amongst several nano-particles plays a key factor on the convective energy transport rate, which is evidently shown in the Figure 4.

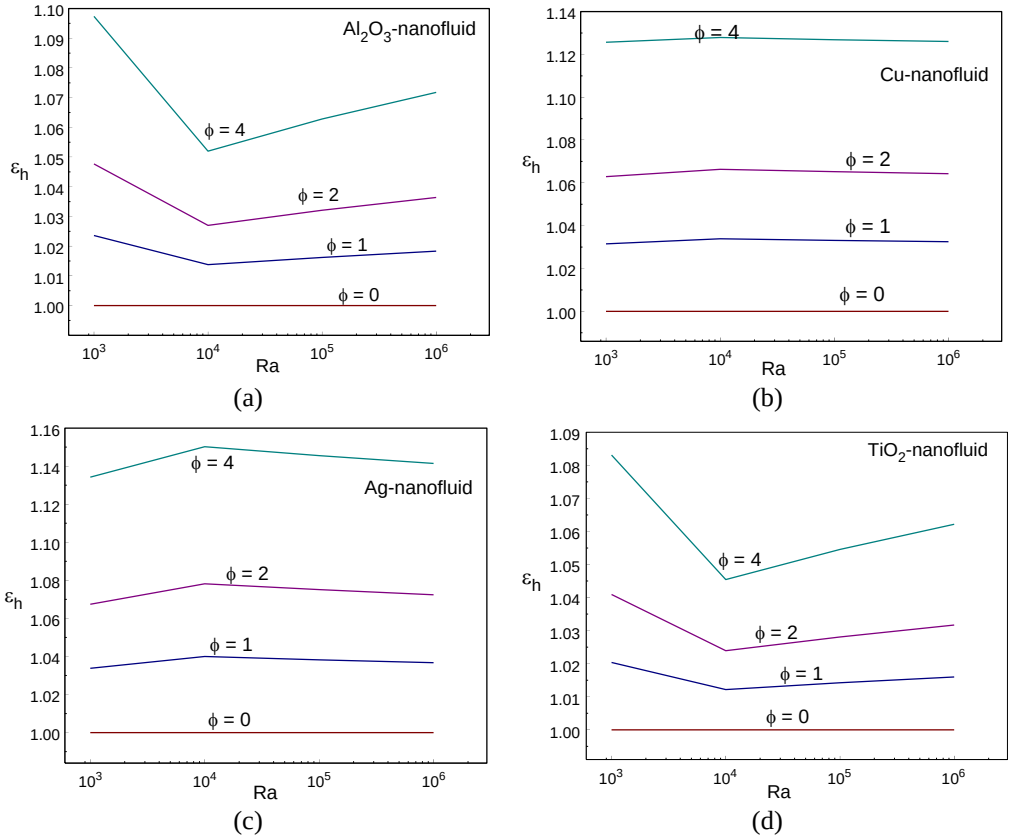

Fig. 5. Heat transfer ratio for different nanofluids.

Figure 5 demonstrated the energy transfer efficacy of the nanoliquid for various volume fraction of the nanoparticle versus Ra. The heat transfer ratio of oxide-nanoliquids (Al_2O_3 & TiO_2) gets minimum when $Ra=10^4$. However, the reverse tendency is detected for using metal nano-particles (Cu and Ag), that is, maximum energy transport rate is achieved at $Ra=10^4$. It is also acquired that energy transport coefficient ratio is higher than one always. It is concluded from these figures that nanoliquids with Al_2O_3 and TiO_2-particle are having similar behaviour while Cu and Ag-nanoliquids are so. The maximum value of the heat transport ratio for the nanoliquids with the oxide particle is attained for $Ra=10^3$ whereas highest value of the heat transfer coefficient ratio for Ag- and Cu-nanoliquids is obtained for $Ra=10^4$. Table 1 shows a significant variance on the averaged Nusselt number for various nano-particles.

4. Final Remarks

The study numerically inspects the heat transfer augmentation of nanoliquids of four different

nanoparticles (Al_2O_3, Cu, Ag and TiO_2) in a rectangular cavity with sinusoidally changing wall temperature. The energy transfer ability of base liquid can be improved when immersing the nano-particles in base fluid and the effect is noticeable as the particle volume fraction increases. However, the growth in averaged Nusselt number is powerfully depending on the nano-particle selected. The heat transfer ratio of Al_2O_3- and TiO_2-nanoliquids is minimum when $Ra=10^4$ while it is high for Cu- and Ag-nanofluid. The nanoliquids with oxide-particles having the similar behaviour on the flow and heat transfer while the nanoliquids with metal particles are having similar trend. A significant variance on the averaged Nusselt number is detected for various nano-particles. The outcomes evidently demonstrate that the type of nanoparticle considered is vital factor on the convective cooling applications.

Table 1. Heat transfer enhancement for different values of ϕ (%) and different nanofluids

Enhancement (%) (A-B)/B×100					
Ra	ϕ (%)	Al_2O_3	TiO_2	Cu	Ag
10^3	1	2.3578345	2.0362916	3.1498564	3.3799499
	2	4.7674217	4.0930196	6.2907442	6.7438742
	4	9.7377374	8.3093928	12.567080	13.425409
10^4	1	1.3770573	1.2174648	3.3874794	4.0003232
	2	2.7013461	2.3919569	6.6296668	7.8183877
	4	5.2004845	4.5435240	12.788564	15.026077
10^5	1	1.6224753	1.4230049	3.3109584	3.8243867
	2	3.2103653	2.8061427	6.5233759	7.5138307
	4	6.2830292	5.4566521	12.689394	14.556959
10^6	1	1.8318063	1.5984382	3.2496021	3.6731750
	2	3.6393797	3.1680655	6.4284496	7.2449994
	4	7.1787521	6.2168752	12.606351	14.142465

References

[1]. Ho C.J., Chen M.W., and Li, Z.W. 2008. *Int. J. Heat Mass Transfer*, 51, 4506-4516.
[2]. Sivasankaran, S., Aasaithambi, T., and Rajan, S. 2010. *Maejo Int. J. Sci. Tech*. 4(3), 468-482.
[3]. Ho, C.J., Liu, W.K., Chang, Y.S., Lin, C.C. 2010. *Int. J. Thermal Sciences*, 49, 1345-1353.
[4]. Ho C.J., Chen D., Yan W.M., Mahian O. 2014. *Int. Commun. Heat Mass Transfer* 57, 22-26.
[5]. Sivasankaran S., Sivakumar V., Prakash P. 2010. *Int. J. Heat Mass Transfer*, 53, 4304-4315.
[6]. Bhuvaneswari M, Sivasankaran S, Kim YJ, 2011, *Numerical Heat Transfer A*, 59, 167-184.
[7]. Sivasankaran S., Malleswaran A., Lee J., Sundar P. 2011. *Int. J. Heat Mass Transfer*, 54, 512-525.
[8]. Sivasankaran S., Bhuvaneswari M. 2013. *Numerical Heat Transfer A*, 63(1), 14-30.
[9]. Sivasankaran S., Pan K.L. 2012. *Numerical Heat Transfer A*, 61(2), 101-121.
[10]. Cheong H.T., Zailan Siri, Sivasankaran S. 2013, Int. Commun. Heat Mass Transfer, 45, 75-85.
[11]. Sivasankaran S., Pan K.L. 2014. Numerical Heat Transfer A, 65, 247-268.
[12]. Janagi, K., Sivasankaran, S., Bhuvaneswari, M., Eswaramurthi, M. 2017. *Int. J. Numerical Methods Heat Fluid Flow*, 27(4), 1000-1014.
[13]. Sivakumar, V., Sivasankaran, S. 2014. J. Applied Mech. Tech. Physics, 55(4), 634-649.
[14]. Cheong H.T., Sivasankaran S., Bhuvaneswari M, 2017. *Int. J. Numerical Methods Heat Fluid Flow*, 27 (2), 287-309.
[15]. Sivasankaran, S., Ananthan, S.S., Abdul Hakeem, A.K. 2016. Scientia Iranica -B Mech Engg, 23(3), 1027-1036.
[16]. Sivasankaran S., Cheong H.T., Bhuvaneswari M., Ganesan, P. 2016. Numerical Heat Transfer A, 69(6), 630-642.